BBAA VI International Colloquium on:
Bluff Bodies Aerodynamics & Applications
Milano, Italy, July, 20-24 2008

AERODYNAMIC CALCULATIONS OF CROSSWIND STABILITY OF A HIGH-SPEED TRAIN USING CONTROL VOLUMES OF ARBITRARY POLYHEDRAL SHAPE

Ben Diedrichs

KTH, Dep. of Aeronautical and Vehicle Engineering, Centre for ECO^2 Vehicle Design
SE−10044 Stockholm, Sweden
Bombardier Transportation, Dep. of Aero- and Thermodynamics
SE−72173 Västerås, Sweden
e-mail:ben.diedrichs@se.transport.bombardier.com

Keywords: Train aerodynamics, crosswind stability, train overturning, CFD, wind tunnel testing, ICE 2, Aerodynamic train model

1 INTRODUCTION

The understanding of crosswind stability for rail cars has matured considerably in the railway community during the last decade. This is partly thanks to the work with the European legislations on Technical Specifications for Interoperability (TSI). Further, the ecological aspects for a sustainable development will continue to put crosswind stability of rail cars into the focus, as reduction of energy consumption hinges on the ability to reduce the stabilizing vehicle weight.

Approval of conventional rail cars with CFD is currently discussed for the European standard EN 14067−6. In this context Reynolds Average Navier Stokes (RANS) modelling will continue to be an important technology to assess the flow fields and aerodynamic load distributions of a crucial car. The strongest reason is that a dozen of flow calculations (yaw angles, defined in Figure 1) may be evaluated to fully determine the stability. Currently, this limitation may exclude cumbersome unsteady numerical methods such as Large Eddy Simulations (LES) and Detached Eddy Simulations (DES), where wind tunnel testing is still economically viable by comparison.

Examples of recent studies of crosswind stability using CFD are found in Diedrichs 2003 [1], Wu 2004 [2], Rolén et al. 2004 [3], Hemida 2006 [4] and Diedrichs et al. 2007 [5]. Amongst these investigators Wu, Rolén et al. and Hemida used a slender model of the critical leading control unit of the German ICE 2 train (class 808) of Deutsche Bahn AG, where the bogies were omitted and the studies were confined to yaw angles of typically $\leqslant 30°$. The model is known as the Aerodynamic Train Model (ATM).

The objectives of the present study are to investigate the more realistic shape of the leading car of the ICE 2 train (cf. Refs. [1, 5]) that includes bogies with adherent wheel axles, partial bogie skirts, plough underneath the front-end and inter-car gap. Here results of high, intermediate and low cruising speeds corresponding to the yaw angles of 20°, 30° and 40° are studied.

The additional geometrical features put more emphasize on the mesh generation where automatic meshing tools may be advantageous. To this end, results are here derived with meshes based on arbitrary polyhedral control volumes (APCV) for both hi- and low-Reynolds number (Re) modelling approaches. Results are compared with a traditionally built very fine hexahedral mesh, and a trimmed hexahedral mesh. Moreover, results are compared with a reference wind tunnel test carried out by Bombardier Transportation, where the comparison includes the static surface pressure at various positions along the train, pressure field adjacent to the car body and aerodynamic integral loads.

Figure 1 illustrates the ICE 2 car model in the open test section of the wind tunnel and the static surface pressure at a yaw angle of 30° obtained from one of the calculations. The experimental and numerical models have identical geometry and Reynolds number of 1.4×10^6 based on a reference length of 3 m and onset flow speed.

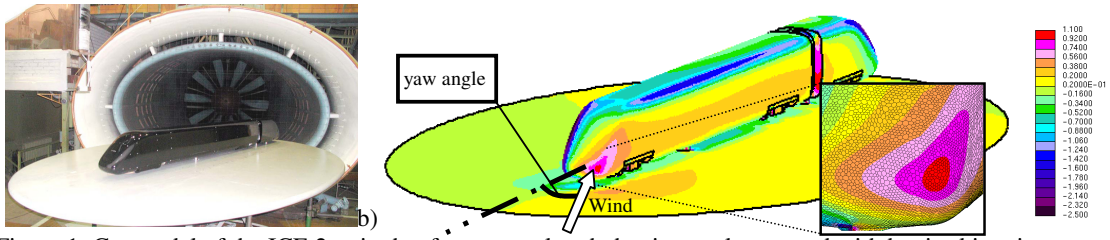

Figure 1: Car model of the ICE 2 train that features a plough, bogies partly covered with bogie skirts, inter-car gap. a) Wind tunnel experiment. b) Calculated surface pressure distribution at 30° and close up of the front-end of the surface mesh utilizing APCV.

2 CALCULATED CASES AND COMPUTATIONAL MESHES

A total number of eight computational meshes are generated, which are listed and described in Table 1. Six meshes are generated for the ICE 2 model (meshes 1–6). Mesh 7 represents a model of ATM that lacks plough and bogies, cf. Ref. [2–4]. Further, in mesh 8 the cylindrical support underneath the test car, discernable in Figure 1, is removed to study the implications of the aerodynamic lift force.

Mesh	Mesh type	Turbulence model	Cells $\times10^6$	Vertices $\times10^6$	Yaw angles	STAR-CD
1. Phc	P	Quadratic $k-\varepsilon$	3	12.9	20,30,40	v4.02
2. Phf	P	Standard $k-\varepsilon$	5	19.5	20,30,40	v4.04
		Quadratic $k-\varepsilon$			20,30,40	
3. Phf2	P	Quadratic $k-\varepsilon$	8.2	34.2	30,40	v4.02
4. Plf	P	$k-\omega$ SST	7.7	26	20,30,40	v4.02
		Quadratic $k-\varepsilon$			30	
5. Th	T	Quadratic $k-\varepsilon$	6.2	6.8	30,40	v4.02
6. Hh	H	Quadratic $k-\varepsilon$	20	20	20,30,40	v3.26
7. Phf –b –p[1)]	P	Quadratic $k-\varepsilon$	4.3	17.9	30,40	v4.02
8. Phf –b –p –c[1,2)]	P	Quadratic $k-\varepsilon$	4.3	17.9	30,40	v4.02

Table 1: Meshes and calculated cases. P = Polyhedral, T = Trimmed H and H = Hexahedral. Phc = [P, hi-Re, coarse]. Phf = [P, hi-Re, fine]. Phf2 = [P, hi-Re, very fine]. Plf = [P, low-Re, very fine]. Th = [T, hi-Re] using the same refinements as Phf2. Hh = [H, hi-Re]. –b = without bogies. –p = without plough. –c = without cylindrical support.

3 LOAD DISTRIBUTION

Central to this investigation is the prediction of the aerodynamic integral loads (defined in EN 14067−1). Figure 2 shows that the largest contributions to the side force are produced on the upper lee-ward (UL) and lower lee-ward (LL) parts of the car body. On the upper wind-ward (UW) part the side force is directed towards the wind, due to the strong suction pressure, shown in Figure 1. Consequently, the crucial lee-rail moment is more forgiving to erroneous predictions in the flow field localized around the UW part as opposed to the UL part. This is also true for the lower wind-ward (LW) part due to the opposite response of the side and lift forces.

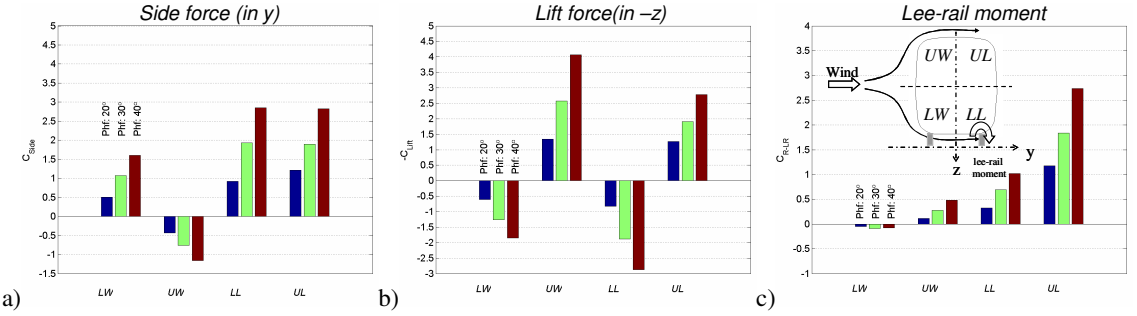

Figure 2: Load distribution of the car body split in four parts regarding the yaw angles of 20°, 30° and 40°. a) Side force, b) lift force and c) crucial moment about the lee-rail (pivotal roll over point).

A discussion of the static surface pressure around the car body of the various calculations and experiment will follow, where data for the 20 m station from the nose are shown in Figure 3. In general, the calculations show fairly coherent results. However, the calculations typically indicate a stronger suction pressure in the underbelly by comparison with the experimental database. This has implications on the lift force which is underestimated. Further, calculations slightly over predict the side force. This altogether results in a crucial lee-rail moment that agrees more satisfactory with the experiments, where the 40° case shows the best comparison. Further, the Hh mesh (see Table 1) returns the best overall agreement with the experiment as far as the lee-rail moment is concerned, where discrepancies are confined to 1.7%, 1.1% and 1.1% for the yaw angles of 20°, 30° and 40°. The corresponding comparison for the Phf mesh yields −1.2%, −5.3% and −3%.

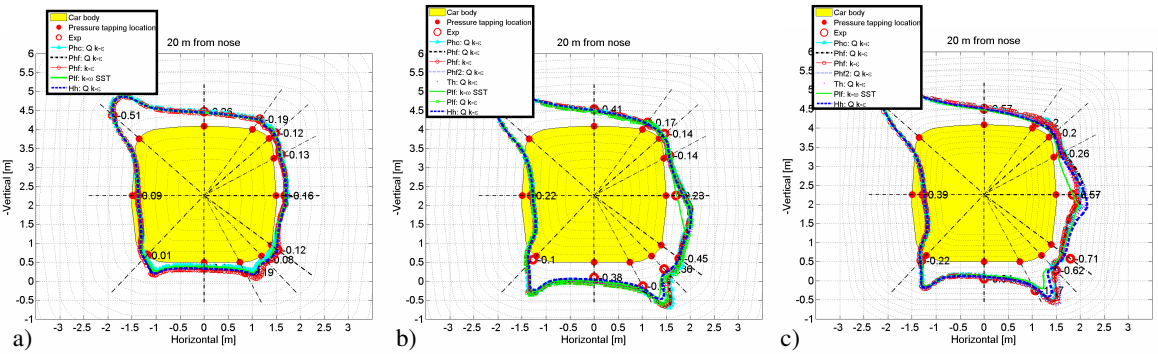

Figure 3: Static pressure around the car body at 20 m from the nose. Yaw angles a) 20°, b) 30° and b) 40°.

The issue with the under predicted lift force has led to new RANS calculations of the ATM, which are carried out with the APCV meshes 7 and 8, see Table 1. Further, a compilation of new and previously calculated results (using technologies of RANS [2, 3], DES [2, 3] and LES [4]) of the ATM concerning the yaw angle of 30° is carried out. The results conclusively indicate a lower lift force compared to the experimental database at our disposal and

show a fair mutual agreement. This suggests that steady state RANS technology is a viable technology for qualification tests as regards the dominant safety issue of crosswind stability for rail cars. To further shed light on this issue a DES of the ICE 2 model is contemplated.

4 CONCLUSIONS

- Automatic meshing utilizing APCV significantly reduces the pre-processing work compared to manual approaches, mitigates the risk of human errors, and typically shortens the total solver time by requiring less iteration on a mesh constructed with fewer cells.
- Steady state RANS approaches appear justified in conjunction with the yaw angles tested here of 20°, 30° and 40°, which correspond to high, intermediate and low cruising speeds.
- The low-Re approaches to represent the near-wall regime around the car body is tested in this study do not seem favorable over the high-Re approaches.
- Lee-rail moment obtains its largest contribution from the upper lee-ward part of the car body. In contrary, the smallest contribution comes from the upper wind-ward part, for which the current geometry is much less sensitive to numerical issues.
- A comparison of current and previous calculated results for the ATM model, shows a consistent trend of under estimating the lift force by comparison with the experimental database. This is likely a result of flow differences adjacent to the ground.
- The current study has concluded the lift force to be very sensitive to geometrical features underneath the train, such as the supporting pillar commonly used in experiments.

ACKNOWLEDGEMENTS

This study is carried out at the Centre for ECO^2 Vehicle Design, a VINNOVA Centre of Excellence at the Royal Institute of Technology (KTH).

REFERENCES

[1] Diedrichs, B. 2003. On computational fluid dynamics modeling of crosswind effects for high-speed rolling stock. *Proc. Instn Mech. Engrs, Part F: J. Rail and Rapid Transit*, **217**(F3), 203–226.

[2] Wu, D. 2004. Predictive Prospects of Unsteady Detached-Eddy Simulations in Industrial External Aerodynamic Flow Simulations. *Final Thesis. Lehrstuhl für Strömungslehre und Aerodynamisches Institute Aachen. Matriculation number: 219949.*

[3] Rolén, C., Rung, T. and Wu, D. 2004. Computational modelling of cross-wind stability of high speed trains. *European Congress on Computational Methods in Applied Sciences and Engineering. ECCOMAS. P. Neittaanmäki, T. Rossi, S. Korotov, E. Oñate, J. Périaux, and D. Knörzer (eds.) Jyväskylä*, 24–28 July.

[4] Hemida, H. 2006. Large-Eddy Simulation of the Flow around Simplified High-Speed Trains under Side Wind Conditions. Thesis for licentiate of engineering no. 2006:06 Chalmers University, Sweden. ISSN 1652-8565.

[5] Diedrichs, B., Sima, M., Orellano, A., and Tengstrand, H. 2007. Crosswind stability of a high-speed train on a high embankment. *Proc. Instn Mech. Engrs, Part F: J. Rail and Rapid Transit*, **221**(F2), 205–225.